Int. J. Heat Mass Transfer. Vol. 27, No. 7, pp. 1087–1097, 1984
Printed in Great Britain

0017 9310/84 $3.00 + 0.00

TRANSITION FROM CONDUCTION TO CONVECTION AROUND A HORIZONTAL CYLINDER EXPERIENCING A RAMP EXCURSION IN INTERNAL HEAT GENERATION

R. E. FAW, R. P. H. ISMUNTOYO† and T. W. LESTER
Nuclear Engineering Department, Kansas State University, Manhattan, KS 66506, U.S.A.

(*Received* 31 *May* 1983 *and in revised form* 14 *October* 1983)

Abstract—The transition from conductive to convective heat transfer has been investigated for horizontal cylinders, platinum wires in various liquids, subjected to internal heat generation increasing linearly with time. Thermal conditions were monitored electrically and transition times were determined from high-speed motion pictures of shadowgraph and interferogram images. Various stability criteria for transition to convection were examined and tested against measurements. For the range of conditions investigated, it was found that the time to transition was inversely proportional to the cube root of the rate of increase in heat generation, and independent of wire diameter.

NOMENCLATURE

- A rate of increase of superficial heat flux
- c fluid heat capacity
- c' cylinder heat capacity
- g acceleration of gravity
- J_n nth order ordinary Bessel function of the first kind
- k fluid thermal conductivity
- k' cylinder thermal conductivity
- K_n nth order modified Bessel function of the second kind
- Nu Nusselt number based on q, $2Rq/k\theta$
- Nu_0 Nusselt number based on q_0, $2Rq_0/k\theta$
- Pr Prandtl number, ν/α
- q heat flux at cylinder surface
- q_0 superficial heat flux, power dissipated per unit cylinder surface
- q^* characteristic heat flux
- Q power dissipated per unit length of cylinder
- r radial distance
- R cylinder radius
- Ra Rayleigh number, $g\beta R^3\theta/\alpha\nu$
- Ra^* Rayleigh number evaluated with $\theta = \theta^*$
- Ra_Δ Rayleigh number evaluated with $R = \Delta$
- s Laplace transform variable
- t time
- t^* characteristic time, R^2/α
- T temperature
- x dimensionless radial distance, r/R
- Y_n nth order ordinary Bessel function of the second kind.

Greek symbols

- α thermal diffusivity, $k/\rho c$
- β coefficient of volumetric expansion
- δ dimensionless penetration depth, Δ/R
- Δ penetration depth
- ζ dimensionless heat flux, q/q^*
- θ temperature difference, $T - T_\infty$
- θ^* characteristic temperature difference, Rq^*/k
- ν kinematic viscosity
- ρ fluid density
- ρ' cylinder density
- τ dimensionless time, t/t^*
- ψ dimensionless temperature difference, θ/θ^*.

Subscripts

- c transition (critical) condition
- w condition at cylinder surface
- ∞ ambient condition.

1. INTRODUCTION

WHEN a cylinder, initially at a uniform temperature equal to that of a static surrounding fluid, is suddenly heated internally, it has been observed that heat transfer to the fluid takes place first by conduction, then by natural convection [1–3]. This paper reports an investigation of the conduction–convection transition for a horizontal cylinder subjected to internal heating at a rate increasing linearly with time—a ramp power excursion. The paper deals specifically with heat transfer during a ramp power excursion from horizontal platinum wires (0.127 and 0.254 mm diameter) to methanol, water, and ethylene glycol. Transition times were determined from both electrical and optical measurements. The paper also deals with a solution to the conduction problem applicable in general to an arbitrary time dependent heating rate and in particular to a ramp power excursion.

The experimental results presented in this paper for a ramp power excursion are for a case not previously studied. The generalized analysis is an extension of a number of more restricted analyses previously appearing in the literature. Transition from conduction to convection, following step application of power to a horizontal cylinder, was studied first by Ostroumov [1]

† Present address: Research Center for Nuclear Techniques, Tamansari 71, Bandung, Indonesia.

in his investigation of transient heat transfer from a 0.1 mm diameter platinum wire to air and various liquids. He found that the time of transition to convection was proportional to $Q^{-0.6}$, where Q is the power delivered to the wire per unit length. Vest and Lawson [2] investigated transient heat transfer to air and water following step application of power to a 0.203 mm diameter tungsten wire. They found that the transition time was proportional to $Q^{-2/3}$. They also found that the transition could be explained in terms of hydrodynamic instability, namely, that transition takes place when the Rayleigh number based on a 'penetration depth' into the heated fluid reaches a critical value. Parsons and Mulligan [3] investigated transient heat transfer following step application of power to 0.030 and 0.127 mm platinum wires in air. They confirmed that the conduction–convection transition could be interpreted in terms of hydrodynamic instability. They too found that $t_c \propto Q^{-2/3}$, but observed that the stability analysis of Vest and Lawson required refinements to account for the heat capacity and thermal conductivity of the heated wire. Parsons and Mulligan [4] also investigated transient heat transfer following step application of power to a finite-diameter horizontal cylinder (6.32 mm diameter steel) in air. They found that, although some local fluid motion took place at the cylinder sides, such motion was insufficient to affect the global transition to convection taking place as a result of instability of the fluid layer at the top of the cylinder.

Conduction heat transfer from a cylindrical heating element, following step application of power, has received considerable attention because of its importance in measurement of thermal conductivity of solids. For the case of an infinite cylinder with finite heat capacity and infinite thermal conductivity, solutions to the conduction problem have been given by Carslaw and Jaeger [5]. Various approximate solutions have been examined by Blackwell [6], and Ritchie and Sakakura [7]. Kierkus *et al.* [8] examined effects of finite cylinder length and established criteria for treating a finite cylinder as though it were infinite. Various numerical solutions for conduction from a cylinder have been provided by Kawamura *et al.* [9].

One-dimensional (1-D) conduction from a thin metallic ribbon has been investigated by Rosenthal and Miller [10] for the case of internal heat generation increasing exponentially with time (exponential excursion). Their solution was based on the assumption of finite heat capacity but infinite thermal conductivity of the ribbon. Johnson *et al.* [11] extended the analysis to account for finite thermal conductivity of the ribbon. They found that, for a platinum 'ribbon' as thick as 5 mm in water, conductivity effects were negligible.

Convection heat transfer following step application of power to a cylindrical heater was investigated by Elliott [12], Gupta and Pop [13], and Katagiri and Pop [14]. Their studies, however, neglected any purely conductive phase and consequently any transition from conduction to convection.

2. ANALYSIS

Consider an infinitely long, solid, horizontal cylinder of radius R, density ρ', heat capacity c', and thermal conductivity k'. The cylinder is surrounded by a fluid of infinite extent with density ρ, heat capacity c, thermal conductivity k, thermal diffusivity $\alpha = k/\rho c$, and kinematic viscosity ν. The fluid coefficient of thermal expansion is β and the acceleration of gravity is g. The cylinder and the fluid are initially at uniform temperature T_∞. Beginning at time $t = 0$, the cylinder is subjected to a time-dependent superficial heat flux $q_0(t)$, defined as the thermal power delivered to the cylinder per unit surface area. The heat flux from the cylinder to the fluid is $q(t)$ and the resulting temperature in the fluid is $T(r,t)$. The temperature excess in the fluid is $\theta(r,t) \equiv T(r,t) - T_\infty$. It is assumed that $k' \gg k$ so that the cylinder has a uniform temperature excess $\theta_w(t) = \theta(R,t)$ and that, for a time following application of power, $\theta(r,t)$ is governed by purely conductive heat transfer in the fluid.

2.1. *Conduction from the heated cylinder to the fluid*

During conduction, $\theta(r,t)$ is governed by the equation

$$\nabla^2\theta = \alpha^{-1}\,\partial\theta/\partial t, \tag{1}$$

along with the initial and boundary conditions

$$\theta(r,t) = 0, \quad t = 0, \quad \text{for all } r, \tag{2}$$

$$\theta(r,t) = 0, \quad r = \infty, \quad \text{for all } r, \tag{3}$$

and, at $r = R$ for all t

$$q_0(t) - \frac{R}{2}\rho' c' \frac{\mathrm{d}\theta_w}{\mathrm{d}t} = -k\frac{\partial\theta}{\partial r}. \tag{4}$$

Equations (1)–(4) may be rendered dimensionless using the following characteristic parameters: $t^* = R^2/\alpha$, $r^* = R$, and $\theta^* = Rq^*/k$. The choice of q^* depends on the form of $q_0(t)$. If, for example, q_0 is constant, then $q^* = q_0$. If $q_0 = At$, where A is a constant, then $q^* = At^*$. Hence, $\tau = t/t^*$, $x = r/R$, $\psi = \theta/\theta^*$, and $\zeta = q/q^*$. Later, a penetration depth $\Delta(t)$ will be defined, along with its dimensionless counterpart $\delta = \Delta/R$. Equations (1) and (4) may now be written as

$$\nabla^2\psi = \partial\psi/\partial\tau, \tag{5}$$

$$\zeta_0 - \frac{\xi}{2}\frac{\mathrm{d}\psi_w}{\mathrm{d}t} = -\frac{\partial\psi}{\partial x}, \quad x = 1, \tag{6}$$

where the Laplacian is in terms of x, and $\xi \equiv \rho' c'/\rho c$.

Laplace transformation of the dimensionless equations and solution of the resulting ordinary differential equation leads to

$$\bar{\psi}(x,s) = \frac{\bar{\zeta}_0(s)K_0(s^{1/2}x)}{(\xi/2)sK_0(s^{1/2}) + s^{1/2}K_1(s^{1/2})}. \tag{7}$$

in which $\bar{\psi}(x,s)$ is the transform of $\psi(x,\tau)$ and K_0 and K_1 are the zero- and first-order modified Bessel functions of the second kind, respectively.

Contour integration, and application of the

convolution integral for Laplace transforms, leads to the following expression for $\psi(x,\tau)$

$$\psi(x,\tau) = -\frac{2}{\pi}\int_0^\infty \frac{du}{f(u)}\Big((\xi/2)u[J_0(u)Y_0(xu) - Y_0(u)J_0(xu)] - [J_1(u)Y_0(xu) - Y_1(u)J_0(xu)]\Big) \times \exp[-u^2\tau]\int_0^\tau d\tau' \exp[u^2\tau']\zeta_0(\tau'), \quad (8)$$

in which

$$f(u) = [(\xi/2)uJ_0(u) - J_1(u)]^2 + [(\xi/2)uY_0(u) - Y_1(u)]^2. \quad (9)$$

The J_n and Y_n functions are the nth order ordinary Bessel functions of the first and second kinds, respectively.

Equation (8) leads to the following expressions for dimensionless cylinder temperature $\psi_w(\tau)$ and dimensionless cylinder-surface heat flux $\zeta(\tau) \equiv -\partial\psi/\partial x|_{x=1}$

$$\psi_w(\tau) = \frac{4}{\pi^2}\int_0^\infty \frac{du}{uf(u)} \exp[-u^2\tau] \times \int_0^\tau d\tau' \exp[u^2\tau']\zeta_0(\tau'), \quad (10)$$

and

$$\zeta(\tau) = -\frac{2}{\pi}\int_0^\infty \frac{du\,u}{f(u)}((\xi/2)u[J_1(xu)Y_0(u) - J_0(u)Y_1(xu)] + [Y_1(xu)J_1(u) - J_1(xu)Y_1(u)]) \times \exp[-u^2\tau]\int_0^\tau d\tau' \exp[u^2\tau']\zeta_0(\tau'). \quad (11)$$

Equations (10) and (11) are generally applicable to the 1-D problem as long as the thermal conductivity of the heater is much greater than that of the surrounding fluid.

The conventional Nusselt number, $Nu(t) \equiv 2Rq(t)/k\theta_w(t)$, can also be written as $Nu(\tau) = 2\zeta/\psi_w$. Similarly, one may define a 'superficial' Nusselt number, Nu_0, in terms of the superficial heat flux, $q_0(t)$, so that $Nu_0(\tau) = 2\zeta_0/\psi_w$. This takes on particularly simple forms for step and ramp power application, namely, $2/\psi_w$ and $2\tau/\psi_w$, respectively.

2.2. *Transition from conduction to convection*

Vest and Lawson [2] have suggested that transition takes place when the Rayleigh number $Ra_\Delta \equiv (g\beta/\alpha\nu)\Delta^3\theta_w$, based on the penetration depth for conduction, Δ, reaches a critical value Ra_c. This hypothesis is supported by their experimental data as it is by the data of Parsons and Mulligan [3], in both instances for step application of power to a cylindrical heater.

The penetration depth $\Delta(t)$ during conduction is defined as the effective radial distance beyond the cylinder surface to which the fluid temperature is influenced. Various models may be used in evaluating $\Delta(t)$. Perhaps the simplest approximates $\theta(r,t)$ as that which would take place as a result of steady conduction between concentric cylinders of radii R and $R+\Delta(t)$, the inner surface being at a temperature excess θ_w over that at the outer. Specifically

$$\theta(r,t) \simeq \theta_w(t)\frac{\ln[r/(R+\Delta)]}{\ln[R/(R+\Delta)]}. \quad (12)$$

This formulation has the advantages of simplicity and satisfaction of the boundary conditions $\theta(R,t) = \theta_w(t)$ and $\theta(R+\Delta,t) = 0$. It has the disadvantage that, because $\partial\theta/\partial r \neq 0$ at $r = R+\Delta$, it does not satisfy the following statement of energy conservation [see equation (4)]

$$q_0(t) - \frac{R}{2}\rho' c'\frac{d\theta_w}{dt} = \frac{\rho c}{R}\frac{d}{dt}\int_R^{R+\Delta} dr\, r\theta(r,t). \quad (13)$$

However, $\Delta(t)$ may be determined very simply by the requirement that, at $r = R$

$$-[2R/\theta_w(t)]\partial\theta/\partial r = Nu(t). \quad (14)$$

In terms of dimensionless variables, $\delta \equiv \Delta/R$ is given by

$$\delta(\tau) = \exp[2/Nu(\tau)] - 1. \quad (15)$$

The formulation of equation (13) may be modified by a quadratic correction in $(r-R)/\Delta$ in order to satisfy the conditions $\theta(R,t) = \theta_w$, and, at $r = R+\Delta$, $\theta = \partial\theta/\partial r = 0$. The result is

$$\theta(r,t) \simeq \theta_w(t)\frac{\Delta/(R+\Delta)}{\ln[R/(R+\Delta)]} \times \left(\frac{r-R}{\Delta} - \frac{(r-R)^2}{\Delta^2} + \frac{(R+\Delta)}{\Delta}\ln[r/(R+\Delta)]\right). \quad (16)$$

This approximation may be used to satisfy equation (13), from which

$$\frac{\delta(2+\delta)(3+2\delta)}{6(1+\delta)\ln(1+\delta)} = \frac{\tau^2}{\psi_w} - \xi. \quad (17)$$

Resulting values of $\delta(\tau)$, of course, do not satisfy equation (15). Nevertheless, based on either equation (15) or equation (17), $\delta(\tau) \propto \tau^{0.52}$ for $1 < \tau < 300$ and $0.68 < \xi < 1.46$.

The requirement that, at transition time t_c, $Ra_\Delta = Ra_c$ can be expressed as

$$\delta^3(\tau_c)\psi_w(\tau_c) = 8Ra_c/Ra^*, \quad (18)$$

where Ra^* is a Rayleigh number based on $\theta^* = Rq^*/k$, namely, $Ra^* = (g\beta/\alpha\nu)(2R)^3\theta^*$. The LHS of equation (18) depends only very weakly on fluid and cylinder properties—through the parameter ξ in equations (11) and (17). The dependence of τ_c on cylinder and fluid properties *and* on the power delivered to the cylinder, is thus embodied essentially in the parameter Ra^*. Using either equation (15) or equation (17), $\delta^3(\tau)\psi_w(\tau) \propto \tau^3$ over $1 < \tau < 300$ and $0.68 < \xi < 1.46$. Thus, from equation (18)

$$\tau_c = C(Ra^*)^{-1/3}, \quad (19)$$

where the unknown critical Rayleigh number is incorporated into the constant C which is independent of fluid and cylinder properties *and* of the rate of heat addition to the cylinder.

The hydrodynamic stability criterion for transition as advanced by Vest and Lawson, may be stated as follows: During the transient-conduction stage, the conductive-penetration depth increases along with the cylinder temperature. Ultimately, the product $\Delta^3\theta_w$, as incorporated in the Rayleigh number, reaches such a value that perturbations are amplified and convection ensues. A similar criterion may be expressed as follows: During transient conduction, the conductive-penetration depth increases along with the cylinder temperature until the depth reaches the average convective-penetration depth that can be sustained at the same cylinder temperature. At that time, convection ensues. In other words, at the transition time

$$Nu_{conv}(\theta_w(t_c)) = Nu_{cond}(t_c). \tag{20}$$

In order to quantify this criterion, we use the Churchill–Chu correlation [15], for laminar convection from a horizontal cylinder with a constant heat flux

$$Nu_{conv} = [0.36 + 0.521F(Pr)]Ra^{1/4}, \tag{21}$$

where

$$Ra = (g\beta/\alpha\nu)(2R)^3\theta_w, F(Pr) = [1 + (0.442/Pr)^{9/16}]^{-4/9},$$

and Pr is the fluid Prandtl number. Since $Ra = Ra^* \psi_w$, the criterion for transition may be written as

$$\frac{[Nu(\tau_c) - 0.36]^4}{\psi_w(\tau_c)} = [0.521F(Pr)]^4 Ra^*. \tag{22}$$

The LHS of this equation depends only very weakly on material properties, through the parameter ξ. As in equation (18), the dependence of τ_c on material properties *and* heating power is embodied in the parameter Ra^*.

3. DESCRIPTION OF APPARATUS AND EXPERIMENTAL PROCEDURE

3.1. *General procedure*

A test cylinder, or heater, in the form of a horizontal platinum wire was suspended in a test fluid—water, methanol, or ethylene glycol. A direct current was applied to the heater in such a way that the power applied, i.e. the superficial heat flux, increased linearly with time. During the power ramp, measurements were made of the current through the heater and the potential change across it. From these measurements, with the platinum serving as a resistance thermometer, the superficial heat flux and the heater temperature could be calculated. Also during the ramp, the heater was illuminated by a beam of laser light used to construct either shadowgram or interferogram images which were recorded photographically. From the photographic records it was possible to determine the time of transition from conductive to convective heat transfer. Details of the procedure may be found in ref. [16] and are summarized below.

3.2. *Test section*

The test fluid was contained in a vessel 11 cm square and 8 cm deep, with walls of 0.25 in. plate glass. This vessel was then placed in an outer insulating enclosure in the form of a 30 cm cube made of 0.25 in. transparent lucite panels. The heater was either 0.127 or 0.254 mm diameter platinum wire (Omega Engineering, Inc.). The nominal length of the heater was 7.5 cm. The ambient temperature within the test fluid was monitored to within ± 0.2°C by a thermocouple, mounted near the heater, connected to an Omega Engineering Model 2176A Digital Thermometer.

The heater was soldered to 0.25 in. diameter copper electrodes, positioned vertically and insulated by a polyethylene spacer block. After soldering, the heater was cleaned in acetone and annealed at red heat, in air, for at least 15 min.

The test vessel was cleaned with detergent and water, then rinsed, first with distilled water and then with the test fluid. After preparation of the vessel, the test fluid was introduced and the heater element placed in position. The entire system was then allowed to equilibrate, a process requiring several hours for water and methanol, and up to 16 h for ethylene glycol.

3.3. *Electrical measurements*

The resistance of the heater at ambient temperature, as well as that of the standard resistor used for current measurement, was determined using a potentiometer method [17] employing a Kiethley Model 155 Microvoltmeter Null Indicator, a Leeds and Northup Model K-3 Potentiometer, and an Epply Laboratories Standard Cell. The standard resistor was a 0.25 Ω, 300 W resistor (Ohmite, Model 79-21) with a negligible temperature coefficient of resistance. The reference resistor used in calibration was a 0.5 Ω, 1% precision resister (Dale, Model RH-25/6721).

Current was supplied to the heater by a 12 V storage battery. Power was controlled by a Darlington amplifier (2N6044) driving two power transistors (SK3037) in parallel. The control voltage to the amplifier was provided by a signal from an analog computer (EAI Model TR-10) shaped so that power delivered to the heater increased linearly with time. Signal shaping requirements were determined by prior measurement of the voltage–power characteristics of the amplifier.

Current to the heater passed first through the standard resistor, R_s, in series. The voltage across the resistor, V_s, was measured during the transient to determine the current $i = V_s/R_s$ through the heater. The voltage, along with the current, yielded both the power delivered to the heater, iV_w, and the heater resistance, $R_w = V_w/i$. From the heater resistance, the heater temperature T(°C) was determined from the relation $R_w(T) = R_w(0)[1 + \alpha T + \beta T^2]$, where $R_w(0)$ is the resistance at 0°C and α and β are temperature

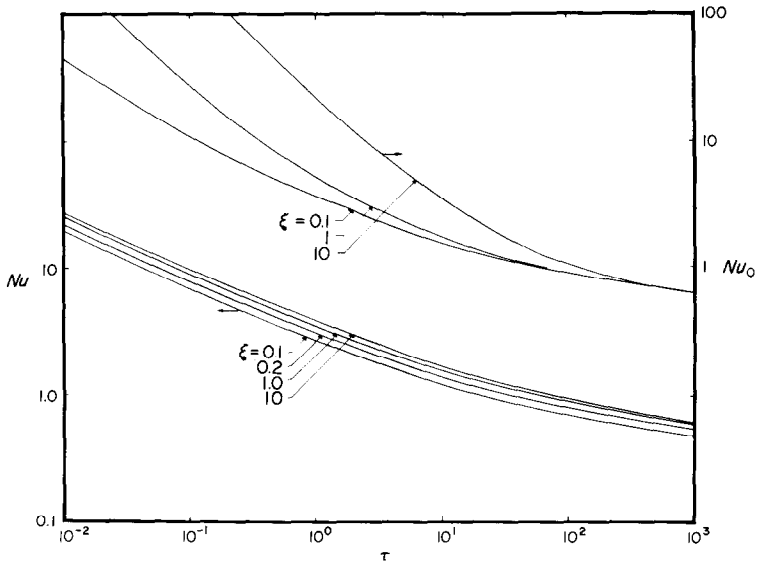

FIG. 1. Nusselt number, Nu, and superficial Nusselt number, Nu_0, as functions of dimensionless time for a ramp power excursion.

coefficients of resistance for platinum. For each heater, $R_w(0)$, α, and β were measured. It was found that measured values of α and β agreed with the published values $\alpha = 0.00392$ and $\beta = -5.5 \times 10^{-7}$ [18].

During a transient, values of V_w and V_s were recorded by a two-channel digital oscilloscope (Nicolet Explorer III). Time steps were selected so that 2048 steps covered the duration of the transient. Voltage precision was 1 part in 4096. Data were first transferred to a floppy disk, and then to a central computer for processing.

3.4. *Optical measurements*

An argon-ion laser (Spectra-Physics Model 165-06), with an air-spaced etalon, was used for both shadowgram and interferogram production. For the former, the horizontal expanded laser beam was directed normal to the heater axis to illuminate a ground-glass plate. For the interferogram, the same beam arrangement, along with a reference beam, was first used to produce a hologram image (object beam) of the fluid and heater using an instant-view holographic 'camera' (Newport Research Instaview Holocamera). During the transient, the hologram beam was superimposed on the reconstructed object beam. Changes in temperature in the fluid, and consequently changes in refractive index, were evidenced as interference patterns in the combined beams.

A high-speed movie camera (Hycam Model 41-0005) was ordinarily used to record either the shadowgram or interferogram images. [In certain instances, a 35 mm still camera (Canon A-1), with motor drive, was substituted.] A switch in the camera, activated when the framing rate reached a constant value, was used to trigger simultaneously the power supply to the heater, the digital oscilloscope, and a shutter in the laser beam. A timing light was operated within the camera, either at 1 or 10 ms intervals. Thus, all measurements were synchronized.

4. RESULTS AND DISCUSSION

4.1. *Conduction solution*

Equations (8), (10) and (11) were integrated numerically for a ramp excursion in superficial heat flux, $\zeta_0(\tau) = \tau$. In each case, for the range $0 \leqslant x \leqslant 0.01$ the integrand was approximated analytically. Trapezoidal integration was used with interval sizes of 0.02 for $0.01 < x \leqslant 5$ and 0.5 for $x > 5$. The error was estimated to be 4% at worst [16]. Results, expressed as

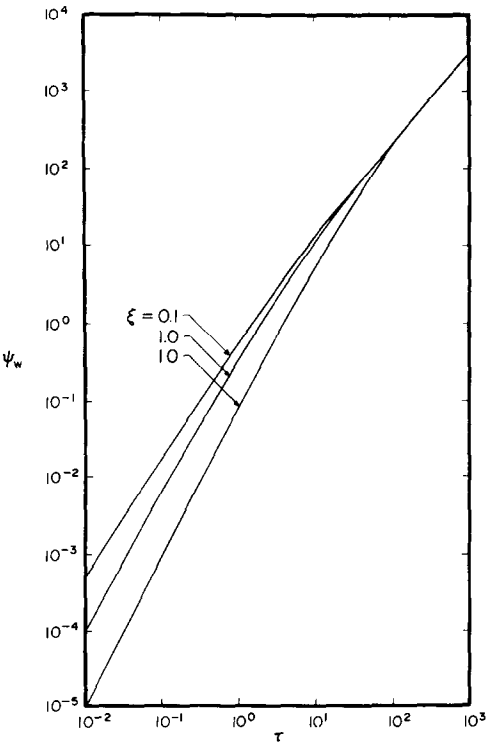

FIG. 2. Dimensionless cylinder temperature, $\psi_w(\tau)$, as a function of dimensionless time for a ramp power excursion.

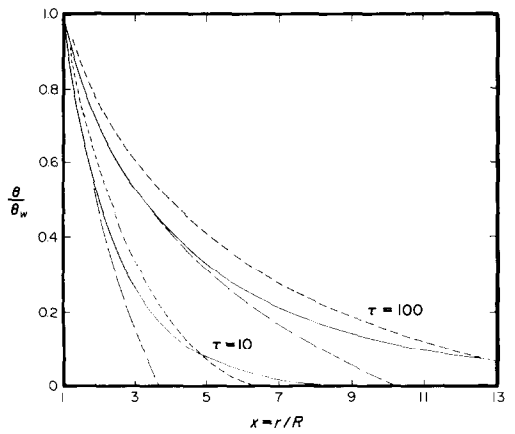

FIG. 3. Dimensionless temperature, $\psi(x, \tau)$, for a ramp power excursion in water ($\xi = 0.688$). The broken lines illustrate profiles based on equations (12) and (15). The dashed lines illustrate profiles based on equations (16) and (17).

$Nu(\tau)$, $Nu_0(\tau)$, and $\psi_w(\tau)$ are shown in Figs. 1 and 2. The radial variation of temperature with time is shown in Fig. 3 for water ($\xi = 0.688$). Also shown in Fig. 3 are approximate profiles based on equations (12) and (16), with corresponding penetration depths evaluated using equations (15) and (17).

4.2. *Electrical measurements*

Measured values of $Nu_0(\tau)$ are shown in Fig. 4 for ramp power excursions in water, methanol, and ethylene glycol. Also shown are conduction solutions. Error bars represent the maximum expected uncertainties (± 3 standard deviations). Uncertainties reflect primarily those for resistance thermometry and are greater at earlier times and lower cylinder temperatures. It is seen that, earlier in the transients, measured values agree well with the conduction solution. During the course of a transient, measured values break away from the conduction solution, indicating a transition to convection heat transfer. Although it is possible to determine transition times from these data, the determination can be done more precisely from results of the optical measurements.

4.3. *Optical measurements*

One series of interferogram photographs was made with the axis of the laser beam parallel to the heater. This was for a 0.254 mm diameter platinum heater in water subjected to a superficial heat flux increasing at a rate of $A = 1000\ \text{W m}^{-2}\ \text{s}^{-1}$. Photographs were made at 2/3 s intervals using a 35 mm still camera and are displayed in Fig. 5. These results are in qualitative agreement with a similar series of photographs made by Vest and Lawson [2]. Early in the series, the radially symmetric interference fringes indicate the conduction mode of heat transfer. After about 2 s a transition to a convective mode of heat transfer is evident.

Shadowgraph results, also photographed using a still camera, are shown in Fig. 6. During the transient, the shadow of the heater broadens due to refraction in the heated fluid. At first, during the conduction phase, the broadening is symmetric about the heater. After transition to convection, which occurs at about 3 s, the image becomes distorted due to the unsymmetric temperature distribution in the fluid about the cylinder.

Sample cine photographs (200 frames s^{-1}) of an interferogram are shown in Fig. 7. The unsymmetric fringe pattern at 800 ms is indicative of transition from conduction to convection.

Measured transition times, τ_c, are given in Table 1. The ramp rates and the Rayleigh numbers have uncertainties (± 3 standard deviations) of $\pm 9\%$. Transition times have maximum uncertainties of $\pm 20\%$. Transition times τ_c are displayed as a function of Ra^* in Fig. 8. The broken line is equation (19), with $C = 14$, the solid lines are from equation (22), with the Prandtl number evaluated at 20°C. Within the precision of these results and the analysis, the transition from conduction to convection is rapid and is described by either of the two related criteria: (1) equality with a

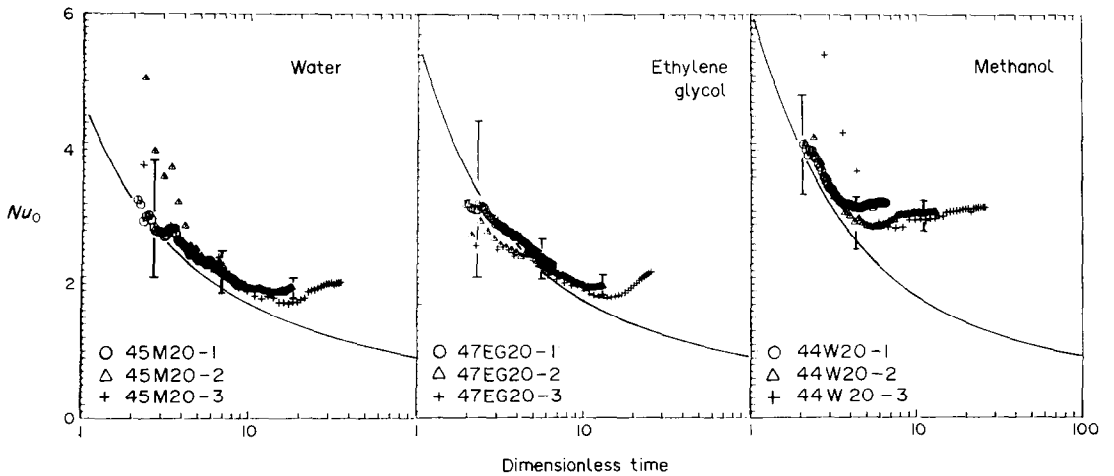

FIG. 4. Measured values of $Nu_0(\tau)$ for: (a) water, (b) ethylene glycol, and (c) methanol. Also shown as solid lines are calculated values of Nu_0 for pure conduction.

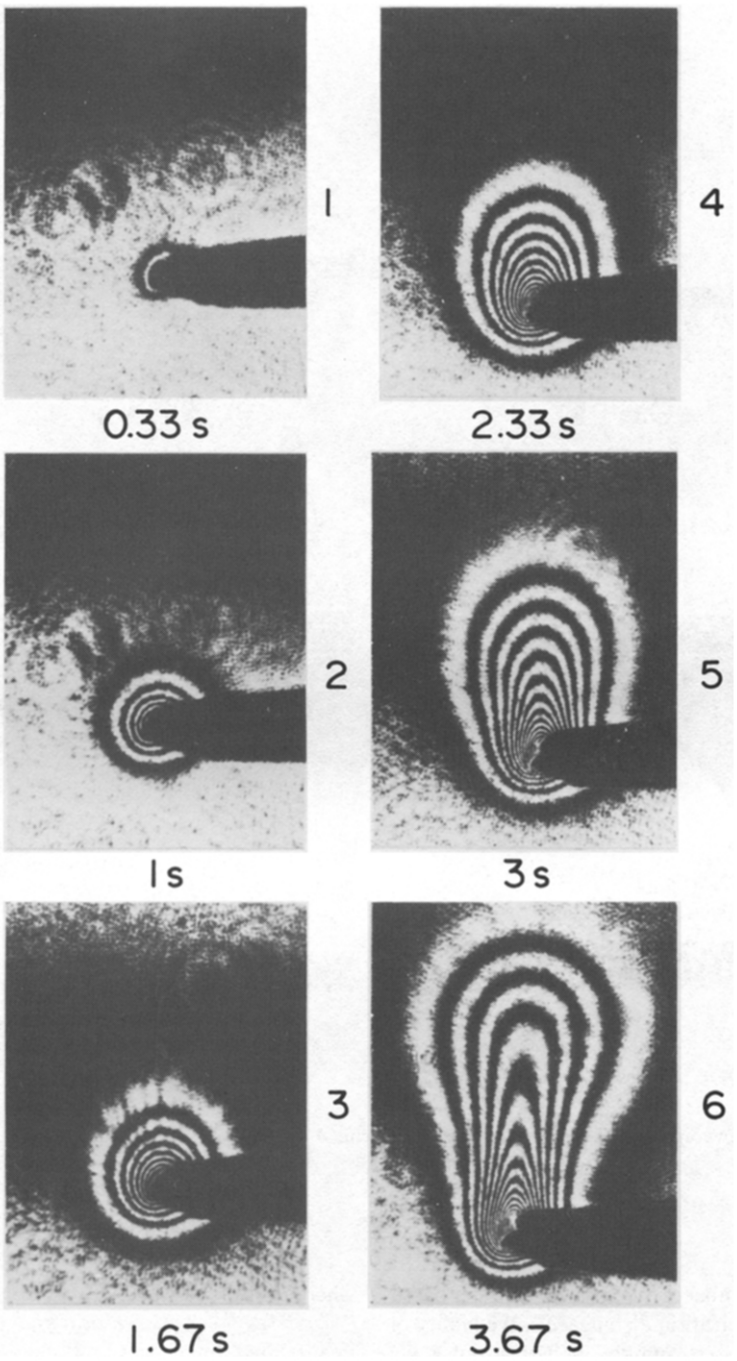

FIG. 5. Interferogram images for a linear power transient ($A = 1000$ W m^{-2} s^{-1}) in a 0.254 mm diameter platinum cylinder in water.

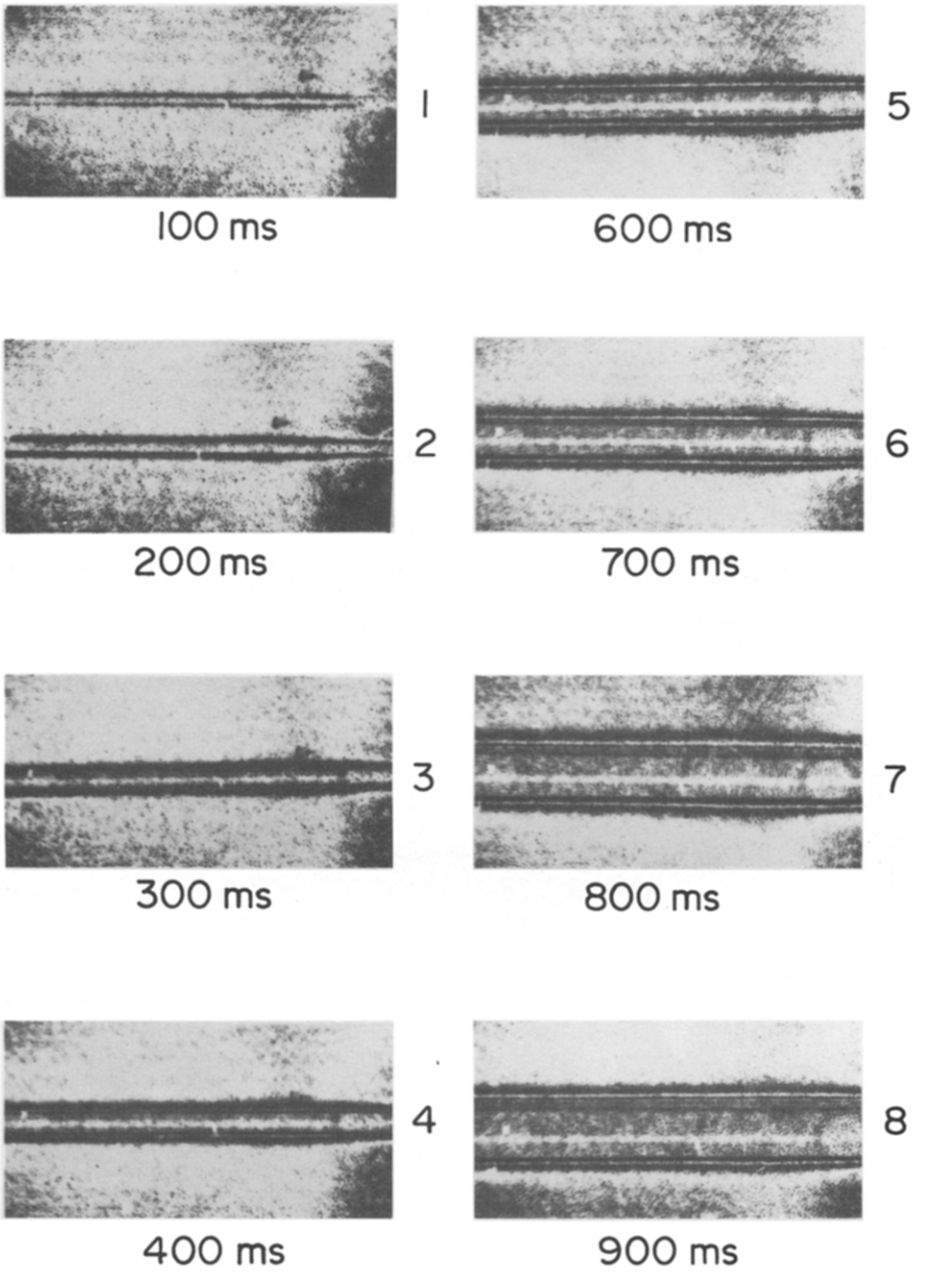

Fig. 6. Shadowgraph images for a linear power transient ($A = 28\,000$ W m^{-2} s^{-1}) in a 0.254 mm diameter platinum cylinder in ethylene glycol.

critical Rayleigh number of the Rayleigh number based on conduction-penetration distance, or (2) equality of the conduction Nusselt number with the convective Nusselt number based on the cylinder wall temperature. It will be noted from Fig. 8 that, empirically, the data are well represented by the relationship $\tau_c \propto (Ra^*)^{-1/3}$. In dimensional variables

$$t_c \propto \left(\frac{\nu k}{\alpha g \beta A}\right)^{1/3},$$

where A is the rate of increase in superficial heat flux (W m^{-2} s^{-1}). Thus, within the range of variables investigated, the transition time is independent of the cylinder radius. It must be noted that the lack of dependence on radius applies to the fine wires employed in this study. As Parsons and Mulligan [4] have found, as the cylinder diameter becomes larger, localized fluid motion takes place at the sides of the cylinder prior to global instability. At some diameter, the concept of a stability-controlled transition to convection may break down.

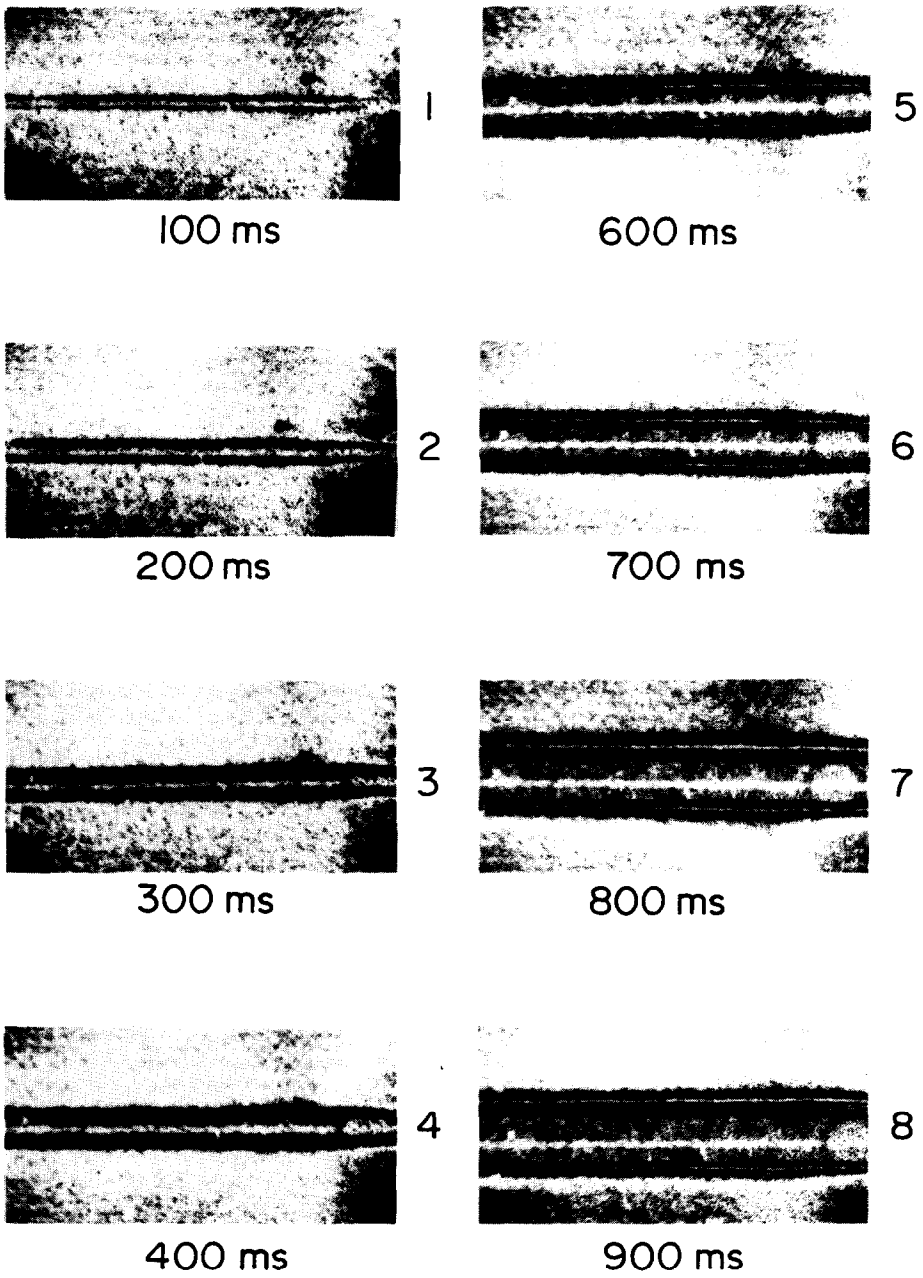

FIG. 7. Interferogram images for a linear power transient ($A = 280\,000$ W m^{-2} s^{-1}) in a 0.127 mm diameter platinum cylinder in ethylene glycol.

5. SUMMARY

In summary, it is noted that a completely general methodology has been developed to analyze the temperature response and surface heat flux of resistive elements with imposed power excursions of arbitrary functional form. This analysis has been used in conjunction with several simplified stability criteria to predict the onset of convection about heating elements undergoing ramp power excursions. The capabilities of the model have been tested against experimental transition times obtained by optical and electrical measurements. Within the range of variables examined, the transition time is well correlated by an expression independent of heater radius; nevertheless, an additional study appears justified to extend the range of heater diameters to more practical values.

Acknowledgements—This work has been supported in part by the National Science Foundation under grant MEA-8102193, and in part by the Nuclear Engineering Department at Kansas State University. The assistance of Mr W. E. Starr, in preparation of apparatus, is gratefully acknowledged.

Table 1. Dimensionless transition time as a function of the Rayleigh number based on the characteristic temperature at the surface of a horizontal platinum cylinder subjected to a ramp increase of superficial heat flux. Physical properties are evaluated at the mean between the ambient fluid temperature (20°C) and the cylinder temperature at the transition time

Fluid	Heater diameter (mm)	A ($W m^{-2} s^{-1}$)	Ra^*	τ_c
Water	0.127	4.2(3)†	2.5(−4)	220
		8.2(3)	1.0(−3)	170
		1.6(4)	2.3(−3)	130
		3.1(4)	5.2(−3)	110
		4.1(4)	7.3(−3)	94
		8.2(4)	1.8(−2)	74
		1.6(5)	4.3(−2)	56
	0.254	4.5(3)	3.6(−2)	47
		8.7(3)	7.5(−2)	36
		9.1(3)	7.2(−2)	19
		1.5(4)	1.2(−1)	19
		1.7(4)	1.7(−1)	28
		4.0(4)	4.9(−1)	21
		4.2(4)	4.3(−1)	15
		8.5(4)	1.1(−0)	13
		9.1(4)	1.5(−0)	16
Ethylene glycol	0.127	1.5(3)	1.1(−4)	240
		3.6(3)	3.1(−4)	190
		8.0(3)	8.0(−4)	140
		1.6(4)	1.7(−3)	96
		2.8(4)	4.2(−3)	86
		6.7(4)	1.3(−2)	54
		1.4(5)	4.8(−2)	43
		2.8(5)	7.9(−2)	23
	0.254	4.6(3)	2.9(−2)	40
		8.9(3)	6.7(−2)	32
		1.8(4)	1.7(−1)	24
		1.9(4)	1.5(−1)	19
		4.4(4)	1.5(−1)	15
		8.7(4)	1.2	10
		9.4(4)	1.7	11
Methanol	0.127	4.1(3)	1.6(−2)	50
		8.1(3)	3.3(−2)	49
		1.6(4)	7.0(−2)	44
		2.7(4)	1.1(−1)	25
		3.8(4)	1.9(−1)	38
		6.0(4)	3.1(−1)	17
		8.0(4)	4.2(−1)	25
		1.4(5)	6.6(−1)	12
		2.8(5)	1.5	10
	0.254	4.4(3)	1.1	12
		4.5(3)	1.2	14
		8.7(3)	2.3	11
		8.8(3)	2.3	11
		1.7(4)	4.5	7.2
		1.7(4)	4.8	10
		4.2(4)	1.2(+1)	4.8
		4.4(4)	1.4(+1)	6.6
		8.2(4)	2.1(+1)	1.9
		8.6(4)	3.1(+1)	6.0

† Read as 4.2×10^3.

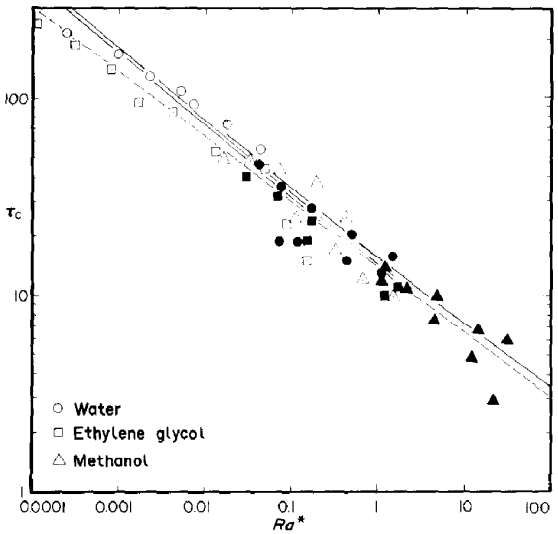

FIG. 8. Dimensionless conduction–convection transition time, τ_c, as a function of the Rayleigh number, Ra^*, based on the cylinder diameter and the characteristic temperature. Open symbols: 0.127 mm diameter cylinder. Closed symbols: 0.254 mm diameter cylinder. The solid lines represent equation (22): upper line, methanol; central line, water; lower line, ethylene glycol. The broken line represents equation (19), with $C = 14$.

REFERENCES

1. G. A. Ostroumov, Unsteady heat convection near a horizontal cylinder, *Soviet Phys. Tech. Phys.* **1**(12), 2627–2641 (1956).
2. C. M. Vest and M. E. Lawson, Onset of convection near a suddenly heated horizontal wire, *Int. J. Heat Mass Transfer* **15**, 1281–1283 (1972).
3. J. R. Parsons, Jr. and J. C. Mulligan, Transient free convection from a suddenly heated horizontal wire, *J. Heat Transfer* **100**, 423–428 (1978).
4. J. R. Parsons, Jr. and J. C. Mulligan, Onset of natural convection from a suddenly heated horizontal cylinder, *J. Heat Transfer* **102**, 636–639 (1980).
5. H. S. Carslaw and J. C. Jaeger, *Conduction of Heat in Solids* (2nd edn.), p. 342. Oxford University Press, Oxford (1959).
6. J. H. Blackwell, A transient-flow-method for determination of thermal constants of insulating materials in bulk, *J. Appl. Phys.* **25**, 137–144 (1954).
7. R. H. Ritchie and A. Y. Sakakura, Asymptotic expansions of solutions of the heat conduction equation in internally bounded cylindrical geometry, *J. Appl. Phys.* **27**, 1453–1459 (1956).
8. W. T. Kierkus, N. Nani and J. E. S. Venart, Radial-axial transient heat conduction in a region bounded internally by a circular cylinder of finite length and appreciable heat capacity, *Can. J. Phys.* **51**, 1182 (1973).
9. H. Kawamura, F. Tachibana and M. Akiyama, Heat transfer and DNB heat flux in transient boiling, IVth Heat Transfer Conf., Paris-Versailles, Paper B3.3 (1970).
10. M. W. Rosenthal and R. L. Miller, An experimental study of transient boiling, Report ORNL-2294, Oak Ridge National Laboratory (1957).
11. H. A. Johnson, V. E. Schrock, F. B. Selph, J. H. Lienhard and Z. R. Rostóczy, Temperature variation, heat transfer, and void volume development in the transient atmospheric boiling of water, Report SAN-1001, Institute of Engineering Research, University of California, Berkeley, California (1961).
12. L. Elliott, Free convection on a two-dimensional axisymmetric body, *Q. Jl Mech. Appl. Math.* **XIII**(2), 153–162 (1970).
13. A. S. Gupta and I. Pop, Effects of curvature on unsteady free convection past a circular cylinder, *Physics Fluids* **20**, 162–163 (1977).

14. M. Katagiri and I. Pop, Transient free convection from an isothermal horizontal circular cylinder, *Wärme- und Stoffübertragung* **12**, 73–81 (1979).
15. S. W. Churchill and H. H. S. Chu, Correlating equations for laminar and turbulent free convection from a horizontal cylinder, *Int. J. Heat Mass Transfer* **18**, 1049–1053 (1975).
16. R. P. H. Ismuntoyo, A study of transient conduction and convection from a heated horizontal cylinder, Ph.D. dissertation, Nuclear Engineering Department, Kansas State University (1982).
17. M. B. Stout, *Basic Electrical Measurements* (2nd edn.), pp. 104, 217. Prentice-Hall, Englewood Cliffs, New Jersey (1960).
18. R. F. Vines, *The Platinum Metals and their Alloys*. International Nickel Co., New York (1941).

TRANSITION DE LA CONDUCTION A LA CONVECTION AUTOUR D'UN CYLINDRE HORIZONTAL SOUMIS A UNE RAMPE DE GENERATION INTERNE DE CHALEUR

Résumé—On étudie la transition de la conduction à la convection thermiques pour des cylindres horizontaux, des fils de platine dans différents liquides, soumis à une génération interne de chaleur qui croît linéairement avec le temps. Les conditions thermiques sont pilotées électriquement et les temps de transition sont déterminés par des prises de vues à grande vitesse d'ombres et d'interférences. Différents critères de stabilité pour la transition à la convection sont examinés et testés par des mesures. Dans le domaine des conditions étudiées, on trouve que le temps de transition est inversement proportionnel à la racine cubique de la vitesse de croissance de la génération de chaleur et indépendant du diamètre du fil.

ÜBERGANG VON WÄRMELEITUNG ZU KONVEKTION UM EINEN HORIZONTALEN ZYLINDER, DESSEN INNERE WÄMEERZEUGUNG ENTSPRECHEND EINER LINEAREN ANSTIEGSFUNKTION ERFOLGT

Zusammenfassung—Der Übergang von Wärmeleitung zu konvektivem Wärmeübergang wurde an horizontalen Zylindern untersucht; im besonderen an Platindrähten in verschiedenen Flüssigkeiten, deren innere Wärmeerzeugung linear mit der Zeit anstieg. Die thermischen Bedingungen wurden auf elektrischem Wege aufgezeichnet, und die Zeiten für den Übergang wurden durch Auswertung von Schattenschlierenbildern und Interferogrammen erhalten. Es wurden verschiedene Stabilitätskriterien für den Übergang zur Konvektion untersucht und mit Messungen verglichen. Die Berechnungen ergaben, daß die Zeit für den Übergang umgekehrt proportional zur dritten Wurzel der Anstiegsgeschwindigkeit der Wärmeerzeugung und unabhängig vom Drahtdurchmesser ist.

ПЕРЕХОД ОТ ТЕПЛОПРОВОДНОСТИ К КОНВЕКЦИИ ВОКРУГ ГОРИЗОНТАЛЬНОГО ЦИЛИНДРА ПРИ ИЗМЕНЕНИИ ВНУТРЕННЕГО ТЕПЛОВЫДЕЛЕНИЯ ПО ЛИНЕЙНОМУ ЗАКОНУ

Аннотация—Проведено исследование перехода от теплопроводности к конвекции для помещаемых в различные жидкости горизонтальных цилиндров в виде платиновых проволочек с внутренним тепловыделением, линейно возрастающим во времени. Нагрев осуществлялся электрическим током, а время перехода определялось с помощью теневой киносъемки и интерферограмм. По результатам измерений проверялись различные критерии конвективной устойчивости. Для диапазона исследованных условий найдено, что время до наступления перехода обратно пропорционально кубическому корню скорости роста тепловыделений и не зависит от диаметра проволоки.